EVALUATION OF LIGHTNING RETURN STROKE CURRENT USING MEASURED ELECTROMAGNETIC FIELDS

M. Izadi[1, *], M. Z. A. Ab Kadir[1], C. Gomes[1], and V. Cooray[2]

[1]Centre of Excellence on Lightning Protection (CELP), Faculty of Engineering, Universiti Putra Malaysia, 43400 UPM, Serdang, Selangor, Malaysia

[2]Division for Electricity, Department of Engineering Sciences, Uppsala University, Uppsala, Sweden

Abstract—The lightning return stroke current is an important parameter for considering the effect of lightning on power lines. In this study, a numerical method is proposed to evaluate the return stroke current based on measured electromagnetic fields at an observation point in the time domain. The proposed method considers all field components and the full wave shape of the current without the use of a special current model as a basic assumption compared to previous methods. Furthermore, the proposed algorithm is validated using measured fields obtained from a triggered lightning experiment. The results show a good agreement between the simulated field based on the evaluated currents from the proposed method and the corresponding measured field at a remote observation point. The proposed method can determine current wave shapes related to a greater number of lightning occurrences compared to the direct measurement of the current.

1. INTRODUCTION

The lightning return stroke current is an important parameter for the evaluation of the effect of lightning on power lines as the lightning can influence a power network both directly and indirectly. For the direct effect, lightning strikes a tower or a power line while an indirect effect is caused by lightning striking the ground or any object around

a power line and a voltage will be induced on the power line by coupling between the electromagnetic fields of the lightning and the line conductors. Several studies have been completed to evaluate the return stroke current which can be categorized into two groups; i.e., direct measurement of the current [1] and inverse procedure algorithms based on measured electromagnetic fields for the determination of the return stroke current [2, 3]. In the direct measurement method, the current can be measured by setting current coils at the top of towers or by using the artificial triggered lightning technique to measure channel base currents [1, 4–6]. On the other hand, indirect methods can evaluate the return stroke current using measured fields and they can cover a greater number of lightning occurrences compared to direct measurement [7]. Different methods are available to evaluate the current although some of these methods only consider the fields measured at a far distance from the lightning channel and ignore the electrostatic and induction components of the fields [7–12]. Furthermore, some methods evaluate the current by using measured fields that are recorded up to intermediate distances from the lightning channel [3, 13–15], although they can only determine the current values at only selected sample frequencies The current model is a basic assumption in these methods. In this study, a general algorithm for the evaluation of the return stroke current using measured electromagnetic fields is proposed which considers the different field components unlike the previous methods. It can also evaluate the full shape of the currents at different heights using an unknown current model based on measured electromagnetic fields. In addition, the proposed method is validated using measured fields obtained from a triggered lightning experiment and the results are discussed accordingly. The basic assumptions in this study are as follows:

1- The lightning channel is a vertical channel on the surface of the ground.
2- The effect of lightning branches on the fields is ignored.
3- The ground conductivity is assumed to be infinity.
4- The surface of the ground is assumed to be flat.

2. RETURN STROKE CURRENT

The return stroke current can be considered in two areas i.e., the channel base current and the currents at different heights along a lightning channel. The channel base current can be simulated using current functions while the constant coefficients of these functions are determined using measured currents. On the other hand, the

current behaviour at different heights along a lightning channel can be modelled via different current models as follows [16]:

1- The gas-dynamic models [17–19].
2- The electromagnetic models [20–22].
3- The distributed circuit models [23–25].
4- The engineering models [26–30].

In this study, the sum of two Heidler functions is selected as a general form of current function as given by Equation (1) [31] while the result of the current evaluation based on the proposed algorithm can be expressed by this function. Therefore, the constant parameters of the current function will be determined using the proposed method based on the measured fields. Noted that the total amplitude of channel base current is dependent on combination of both Heidler functions.

$$i\left(0,t\right)=\frac{i_{01}}{\eta_1}\frac{\left(\frac{t}{\Gamma_{11}}\right)^{n_1}}{1+\left(\frac{t}{\Gamma_{11}}\right)^{n_1}}\exp\left(\frac{-t}{\Gamma_{12}}\right)+\frac{i_{02}}{\eta_2}\frac{\left(\frac{t}{\Gamma_{21}}\right)^{n_2}}{1+\left(\frac{t}{\Gamma_{21}}\right)^{n_2}}\exp\left(\frac{-t}{\Gamma_{22}}\right) \quad (1)$$

where:

i_{01}/i_{02} is the current amplitude of first/second Heidler function in Equation (1),

Γ_{11}/Γ_{12} is the front time constant of first/second Heidler function in Equation (1),

Γ_{21}/Γ_{22} is the decay-time constant in first/second Heidler function in Equation (1),

n_1, n_2 are the exponents with values 2–10 usually taken,

$$\eta_1 = \exp\left[-\left(\Gamma_{11}/\Gamma_{12}\right)\left(n_1\times\frac{\Gamma_{12}}{\Gamma_{11}}\right)^{\frac{1}{n_1}}\right],$$

$$\eta_2 = \exp\left[-\left(\Gamma_{21}/\Gamma_{22}\right)\left(n_2\times\frac{\Gamma_{22}}{\Gamma_{21}}\right)^{\frac{1}{n_2}}\right].$$

Furthermore, the general form of the engineering current models is set for consideration of the current behaviour at different heights along a lightning channel as expressed in Equation (2) while the attenuation height dependent factors are the unknown parameters that can be determined by the proposed method [16, 32–34]

$$I\left(z',t\right) = I\left(0,t-\frac{z'}{v}\right)\times P(z')\times u\left(t-\frac{z'}{v_f}\right) \quad (2)$$

where:

z' is the temporary charge height along lightning channel,

$I(z', t)$ is current distribution along lightning channel at any height z' and any time t,

$I(0, t)$ is channel base current,

$P(z')$ is the attenuation height dependent factor,

v is the current-wave propagation velocity,

v_f is the upward propagating front velocity,

u is the Heaviside function defined as $u(t - \frac{z'}{v_f}) = \begin{cases} 1 & \text{for } t \geq \frac{z'}{v_f} \\ 0 & \text{for } t < \frac{z'}{v_f} \end{cases}$

3. THE ELECTROMAGNETIC FIELDS ASSOCIATED WITH A LIGHTNING CHANNEL

The electromagnetic fields due to a lightning channel at an observation point above the surface of the ground can be evaluated by Equations (3) and (4) based on the geometry of the problem as illustrated in Figure 1 [35]. Therefore, the magnetic flux density and the vertical electric field can be evaluated by linear expressions directly in the time domain without needing to apply any extra conversions. In this method the lightning channel is divided into a number of sub channels at different steps of Δt based on variation of charge height along real and image channels while the length of each sub channel in real and image channels is evaluated by Δh and $\Delta h'$, respectively. Likewise,
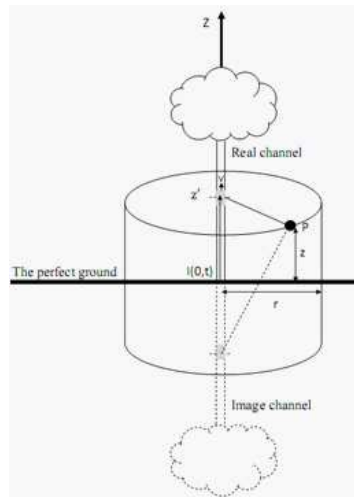

Figure 1. The geometry of lightning channel with respect to observation point.

each sub channel is divided into a number of subparts (k) and the electromagnetic fields are evaluated by combination these sub channels and subparts using Trapezoid and FDTD methods. Therefore, the accuracy of results has an inverse relationship with the value of Δt and a direct relationship with the value of k parameter. However with the increase of accuracy, the processing time will also be longer.

$$B_\varphi(r,z,t_n) = \sum_{i=1}^{n} \sum_{m=1}^{k+1} \left[a_m F_{i,1}(r,z,t_n,h_{m,i}) - a'_m F_{i,1}(r,z,t_n,h'_{m,i}) \right] \quad (3)$$

$$E_z(r,z,t_n) = E_z(r,z,t_{n-1}) + \Delta t \times \sum_{i=1}^{n} \sum_{m=1}^{k+1}$$
$$\left[a_m F_{i,2}(r,z,t_n,h_{m,i}) - a'_m F_{i,2}(r,z,t_n,h'_{m,i}) \right] \quad (4)$$

$$\frac{dE_z(r,z,t_n)}{dt} = \sum_{i=1}^{n} \sum_{m=1}^{k+1} \left[a_m F_{i,2}(r,z,t_n,h_{m,i}) - a'_m F_{i,2}(r,z,t_n,h'_{m,i}) \right] \quad (5)$$

where:

r is the radial distance from lightning channel,

z is the height of observation point with respect to ground surface,

B_φ is the magnetic flux density due to lightning channel,

E_z is the vertical electric field due to lightning channel,

$\frac{dE_z}{dt}$ is the derivative of vertical electric field to time,

c is the light speed in free space,

ε_0 is the permittivity of free space,

μ_0 is the permeability of free space,

$n_{\max}$ is maximum number of time steps,

Δt is time step,

$$\beta = \frac{v}{c}$$

$$\chi = \sqrt{\frac{1}{1-\beta^2}},$$

$$t_n = \frac{\sqrt{r^2+z^2}}{c} + (n-1)\Delta t \quad n = 1,2,\dots n_{\max}$$

$$\Delta h_i = \begin{cases} \beta\chi^2 \left\{ (ct_i - ct_{i-1}) - \sqrt{(\beta ct_i - z)^2 + \left(\frac{r}{\chi}\right)^2} + \sqrt{(\beta ct_{i-1} - z)^2 + \left(\frac{r}{\chi}\right)^2} \right\} & \text{for } i>1 \\ \beta\chi^2 \left\{ -(\beta z - ct_i) - \sqrt{(\beta ct_i - z)^2 + \left(\frac{r}{\chi}\right)^2} \right\} & \text{for } i=1 \end{cases}$$

$$\Delta h'_i = \begin{cases} \beta\chi^2 \left\{ (ct_{i-1} - ct_i) + \sqrt{(\beta ct_i + z)^2 + \left(\frac{r}{\chi}\right)^2} - \sqrt{(\beta ct_{i-1} + z)^2 + \left(\frac{r}{\chi}\right)^2} \right\} & \text{for } i>1 \\ \beta\chi^2 \left\{ -(\beta z + ct_i) + \sqrt{(\beta ct_i + z)^2 + \left(\frac{r}{\chi}\right)^2} \right\} & \text{for } i=1 \end{cases}$$

$$h_{m,i} = \begin{cases} \frac{(m-1)\times\Delta h_i}{k} + h_{m=k+1,i-1} \\ \frac{(m-1)\times\Delta h_i}{k} \end{cases} \quad \text{for } i = 1$$

$$h'_{m,i} = \begin{cases} \frac{(m-1)\times\Delta h'_i}{k} + h'_{m=k+1,i-1} \\ \frac{(m-1)\times\Delta h'_i}{k} \end{cases} \quad \text{for } i = 1$$

$$R = \sqrt{r^2 + (z - h_{m,i})^2}$$

$$F_{i,1}(r, z, t_n, h_{m,i})$$
$$= \left(\frac{\mu_0}{4\pi}\right)\left\{\frac{r}{R^3}i\left(h_{m,i}, t_n - \frac{R}{c}\right) + \frac{r}{c\times R^2}\frac{\partial i\left(h_{m,i}, t_n - \frac{R}{c}\right)}{\partial t}\right\}$$

$$F_{i,2}(r, z, t_n, h_{m,i})$$
$$= \left(\frac{1}{4\pi\varepsilon_0}\right)\left\{\frac{2(z - h_{m,i})^2 - r^2}{R^5}\times i\left(h_{m,i}, t_n - \frac{R}{c}\right) + \frac{2(z - h_{m,i})^2 - r^2}{c\times R^4}\right.$$
$$\left.\times\frac{\partial i\left(h_{m,i}, t_n - \frac{R}{c}\right)}{\partial t} - \frac{r^2}{c^2\times R^3}\times\frac{\partial^2 i\left(h_{m,i}, t_n - \frac{R}{c}\right)}{\partial t^2}\right\}$$

$$a_m = \begin{cases} \frac{\Delta h_i}{2\times k} & \text{for } m = 1 \text{ or } m = k+1 \\ \frac{\Delta h_i}{k} & \text{for others} \end{cases}$$

$$a'_m = \begin{cases} \frac{\Delta h'_i}{2\times k} & \text{for } m = 1 \text{ or } m = k+1 \\ \frac{\Delta h'_i}{k} & \text{for others} \end{cases}$$

k is division factor $(>= 2)$

Figure 2. The geometry of the required field sensors in the proposed method.

4. EVALUATION OF RETURN STROKE CURRENT USING MEASURED ELECTROMAGNETIC FIELDS

The return stroke current at different heights is evaluated using measured electromagnetic fields at an observation point as shown in Figure 2. It is important to mention that the measured fields are collected from a triggered lightning experiment that took place in Florida, USA.

Figure 2 shows that the observation point is located on the ground surface. Therefore, the temporary charge heights at both real and image channels are same as the effect of moving charge in the real and image channels on the observation point are equal and they can be considered by doubling the effect of real channel. Thus, Equations (3), (4) and (5) can be simplified by Equations (6), (7) and (8), respectively.

$$B_\varphi\left(r, z = 0, t_n\right) = \sum\nolimits_{i=1}^{n} \sum\nolimits_{m=1}^{k+1} \{2a_m F_{i,1}\left(r, z = 0, t_n, h_{m,i}\right)\} \qquad (6)$$

$$E_z\left(r, z = 0, t_n\right) = E_z\left(r, z = 0, t_{n-1}\right)$$
$$+\Delta t \times \sum\nolimits_{i=1}^{n} \sum\nolimits_{m=1}^{k+1} \{2a_m F_{i,2}\left(r, z = 0, t_n, h_{m,i}\right)\} (7)$$

$$\frac{dE_z\left(r, z = 0, t_n\right)}{dt} = \sum\nolimits_{i=1}^{n} \sum\nolimits_{m=1}^{k+1} \{2a_m F_{i,2}\left(r, z = 0, t_n, h_{m,i}\right)\}. \qquad (8)$$

Therefore, the required equation system can be expressed by Equation (9) while Equations (6) to (8) are applied at the observation point for $n_{\max}$ samples of electromagnetic fields where $n_{\max}$ is the maximum number of time steps as follows:

$$
\begin{cases}
\vec{B}_\varphi\left(r, z = 0, t_1\right) = \sum_{m=1}^{k+1} \{2a_m F_{i,1}\left(r, z = 0, t_1, h_{m,i}\right)\} \\
\vec{B}_\varphi\left(r, z = 0, t_2\right) = \sum_{i=1}^{2} \sum_{m=1}^{k+1} \{2a_m F_{i,1}\left(r, z = 0, t_2, h_{m,i}\right)\} \\
\vdots \\
\vec{B}_\varphi\left(r, z = 0, t_{n_{\max}}\right) = \sum_{i=1}^{n_{\max}} \sum_{m=1}^{k+1} \{2a_m F_{i,1}\left(r, z = 0, t_{\max}, h_{m,i}\right)\} \\
\vec{E}_z\left(r, z = 0, t_1\right) = \Delta t \times \sum_{m=1}^{k+1} \{2a_m F_{i,2}\left(r, z = 0, t_1, h_{m,i}\right)\} \\
\vec{E}_z\left(r, z = 0, t_2\right) = E_z\left(r, z = 0, t_1\right) + \Delta t \times \sum_{i=1}^{1} \sum_{m=1}^{k+1} \{2a_m F_{i,2}\left(r, z = 0, t_2, h_{m,i}\right)\} \\
\vdots \\
\vec{E}_z\left(r, z = 0, t_{n_{\max}}\right) = E_z\left(r, z = 0, t_{\max-1}\right) + \Delta t \times \sum_{i=1}^{n_{\max}} \sum_{m=1}^{k+1} \\
\qquad \{2a_m F_{i,2}\left(r, z = 0, t_{\max}, h_{m,i}\right)\} \\
\frac{\overrightarrow{dE_z}\left(r, z=0, t_1\right)}{dt} = \sum_{m=1}^{k+1} \{2a_m F_{i,2}\left(r, z = 0, t_1, h_{m,i}\right)\} \\
\frac{\overrightarrow{dE_z}\left(r, z=0, t_2\right)}{dt} = \sum_{i=1}^{2} \sum_{m=1}^{k+1} \{2a_m F_{i,2}\left(r, z = 0, t_2, h_{m,i}\right)\} \\
\vdots \\
\frac{\overrightarrow{dE_z}\left(r, z=0, t_{n_{\max}}\right)}{dt} = \sum_{i=1}^{n_{\max}} \sum_{m=1}^{k+1} \{2a_m F_{i,2}\left(r, z = 0, t_{\max}, h_{m,i}\right)\}
\end{cases}
\qquad (9)
$$

By setting the k factor at 2 in Equation (9), the values of the attenuation factors $(P(z'))$ at different heights along the lightning channel will be unknown parameters whereby the attenuation factors have a great influence on the terms $F_{i,1}$ and $F_{i,2}$ in Equation (9). Therefore, by entering the general form of current function from Equation (1) for the $F_{i,1}$ and $F_{i,2}$ terms of Equation (9) as a basic assumption, six unknown current parameters (i_{01} i_{02}, τ_{11}, τ_{12}, τ_{21}, τ_{22}) will be evaluated by using the measured electromagnetic fields when $n_1 = n_2 = 2$. Moreover, the average value of the return stroke velocity along the lightning channel is an unknown parameter in this algorithm.

Furthermore, the number of unknown attenuation height dependent factors in each one of the vertical electric field and magnetic flux density expressions will be $2 \times n_{\max}$. Therefore, by substituting the measured values of the magnetic flux density, the vertical eclectic field and the derivative of the vertical electric field with respect to time into the left side of each field expression in Equation (9), and shifting the left side of the field expressions to the right side, Equation (9) can be converted to Equation (1) while the measured derivative of the vertical electric field with respect to time can be evaluated by using the measured vertical electric field and using the 2nd finite-difference time-domain (FDTD) method [36–38].

$$
\begin{cases}
\sum_{m=1}^{k+1}\left\{2a_m F_{i,1}\left(r,z=0,t_1,h_{m,i}\right)\right\} - B_\varphi^{(m)}\left(r,z=0,t_1\right)=0 \\
\sum_{i=1}^{2}\sum_{m=1}^{k+1}\left\{2a_m F_{i,1}\left(r,z=0,t_2,h_{m,i}\right)\right\} - B_\varphi^{(m)}\left(r,z=0,t_2\right)=0 \\
\vdots \\
\sum_{i=1}^{n_{\max}}\sum_{m=1}^{k+1}\left\{2a_m F_{i,1}\left(r,z=0,t_{\max},h_{m,i}\right)\right\} - B_\varphi^{(m)}\left(r,z=0,t_{n_{\max}}\right)=0 \\
\Delta t \times \sum_{m=1}^{k+1}\left\{2a_m F_{i,2}\left(r,z=0,t_1,h_{m,i}\right)\right\} - E_z^{(m)}\left(r,z=0,t_1\right)=0 \\
E_z\left(r,z=0,t_1\right) + \Delta t \times \sum_{i=1}^{2}\sum_{m=1}^{k+1}\left\{2a_m F_{i,2}\left(r,z=0,t_2,h_{m,i}\right)\right\} \\
\quad - E_z^{(m)}\left(r,z=0,t_2\right)=0 \\
\vdots \\
E_z\left(r,z=0,t_{\max-1}\right) + \Delta t \times \sum_{i=1}^{n_{\max}}\sum_{m=1}^{k+1} \\
\left\{2a_m F_{i,2}\left(r,z=0,t_{\max},h_{m,i}\right)\right\} - E_z^{(m)}\left(r,z=0,t_{n_{\max}}\right)=0 \\
\sum_{m=1}^{k+1}\left\{2a_m F_{i,2}\left(r,z=0,t_1,h_{m,i}\right)\right\} - \frac{dE_z^{(m)}(r,z=0,t_1)}{dt}=0 \\
\sum_{i=1}^{2}\sum_{m=1}^{k+1}\left\{2a_m F_{i,2}\left(r,z=0,t_2,h_{m,i}\right)\right\} - \frac{dE_z^{(m)}(r,z=0,t_2)}{dt}=0 \\
\vdots \\
\sum_{i=1}^{n_{\max}}\sum_{m=1}^{k+1}\left\{2a_m F_{i,2}\left(r,z=0,t_{\max},h_{m,i}\right)\right\} - \frac{dE_z^{(m)}\left(r,z=0,t_{n_{\max}}\right)}{dt}=0
\end{cases}
\tag{10}
$$

where:

$B_\varphi^{(m)}(r,z=0,t_n)$ is the measured magnetic flux density at time t_n,

$E_z^{(m)}(r,z=0,t_n)$ is the measured vertical electric field at time t_n,

$\frac{dE_z^{(m)}(r,z=0,t_n)}{dt}$ is the derivative of vertical electric field to time at t_n.

The values of the unknown parameters in Equation (10) will be $2 \times n_{\max} + 7$ whereby six parameters are for the current and one parameter is for the return stroke velocity and $2 \times n_{\max}$ parameters are for the attenuation height dependent factors at different heights along the lightning channel. Therefore, in order to reduce the error due to applying the 2nd FDTD method on the vertical electric field for the evaluation of the measured $\frac{dE_z}{dt}$, the seven last equations of $\frac{dE_z}{dt}$ can be entered into the calculations whereby the value of $\frac{dE_z}{dt}$ at later time periods is lower than for earlier time periods. Thus, Equation (10) can be reduced to a nonlinear equation system with $2 \times n_{\max} + 7$ equations and $2 \times n_{\max} + 7$ unknown parameters as follows:

$$
\begin{cases}
\sum_{m=1}^{k+1} \{2a_m F_{i,1}(r,z=0,t_1,h_{m,i})\} - B_\varphi^{(m)}(r,z=0,t_1) = 0 \\
\sum_{i=1}^{2}\sum_{m=1}^{k+1} \{2a_m F_{i,1}(r,z=0,t_2,h_{m,i})\} - B_\varphi^{(m)}(r,z=0,t_2) = 0 \\
\vdots \\
\sum_{i=1}^{n_{\max}}\sum_{m=1}^{k+1} \{2a_m F_{i,1}(r,z=0,t_{\max},h_{m,i})\} - B_\varphi^{(m)}(r,z=0,t_{n_{\max}}) = 0 \\
\Delta t \times \sum_{m=1}^{k+1}\{2a_m F_{i,2}(r,z=0,t_1,h_{m,i})\} - E_z^{(m)}(r,z=0,t_1) = 0 \\
E_z(r,z=0,t_1) + \Delta t \times \sum_{i=1}^{2}\sum_{m=1}^{k+1}\{2a_m F_{i,2}(r,z=0,t_2,h_{m,i})\} \\
\quad - E_z^{(m)}(r,z=0,t_2) = 0 \\
\vdots \\
E_z(r,z=0,t_{\max-1}) + \Delta t \times \sum_{i=1}^{n_{\max}}\sum_{m=1}^{k+1}\{2a_m F_{i,2}(r,z=0,t_{\max},h_{m,i})\} \\
\quad - E_z^{(m)}(r,z=0,t_{n_{\max}}) = 0 \\
\sum_{i=1}^{n_{\max}-6}\sum_{m=1}^{k+1}\{2a_m F_{i,2}(r,z=0,t_{\max-6},h_{m,i})\} - \frac{dE_z^{(m)}(r,z=0,t_{\max-6})}{dt} = 0 \\
\sum_{i=1}^{n_{\max}-5}\sum_{m=1}^{k+1}\{2a_m F_{i,2}(r,z=0,t_{\max-5},h_{m,i})\} - \frac{dE_z^{(m)}(r,z=0,t_{\max-5})}{dt} = 0 \\
\vdots \\
\sum_{i=1}^{n_{\max}}\sum_{m=1}^{k+1}\{2a_m F_{i,2}(r,z=0,t_{\max},h_{m,i})\} - \frac{dE_z^{(m)}(r,z=0,t_{n_{\max}})}{dt} = 0
\end{cases} \tag{11}
$$

Equation (11) can be solved by using the Particle Swarm Optimization (PSO) method [39–47] where each expression in Equation (11) is minimized at the roots of the equation. The PSO searching mechanism is based on the social behavior of a flock of flying birds during their search for food while the position and velocity of the swarm particles are strangely depend on the cooperative communication among all the particles and each individual's own experience at the same time. In order to minimize the function, each PSO particle represents a candidate potential solution with a velocity vector v and a position vector x_i. Therefore, for a swarm of y-particles flying in R^n hyperspace the velocity and position vectors can be expressed by Equations (12)

and (13), respectively as follow;

$$S_i = [x_1^i x_2^i \ldots x_n^i] \quad \text{for } i = 1, 2, \ldots, y \tag{12}$$

$$v = [v_1 v_2 \ldots v_y] \tag{13}$$

where:

i is the particle index,

v is the swarm velocity vector,

n is the optimization problem dimension.

Therefore, the new position of particle can be expressed by previous location and the velocity as given by Equation (14).

$$S_i^{k+1} = S_i^k + v_i^{k+1} \tag{14}$$

where:

S_i^{k+1} is the particle i in new position at iteration $k + 1$,

S_i^k is the particle i in old position at iteration k,

v_i^{k+1} is the particle i with new velocity at iteration $k + 1$.

Moreover, the velocity update vector related to particle I is presented by Equation (15) as follow;

$$v_i^{k+1} = w \times v_i^k + c_1 \times r_1 \times \left(Pbest_i^k - S_i^k \right) + c_2 \times r_2 \times \left(gbest_i^k - S_i^k \right) \tag{15}$$

where:

v_i^k is the previous velocity of particle i,

w is the inertia weight,

c_1, c_2 are the individual and social acceleration positive constants,

r_1, r_2 are the random values in the range [0, 1], sampled from a uniform distribution,

$Pbest_i^k$ is the personal best position associated with particle i own experience,

$gbest_i^k$ is the global best position associated with the whole neighborhood experience.

Thus, the velocity updating is more depend on three major components:

(i) The velocity in previous step and the inertia factor (w).

(ii) The individual's own experience of particle (cognitive component).

(iii) The intelligent exchange of information between particle i and the swarm (social component).

In this paper, each expression of Equation (11) is set as an objective function and the whole system is considered as a multi objective case where the equations are minimized at the roots. Moreover, the values of c_1, c_2 and w are set at 2, 2 and 1, respectively. The proposed method can evaluate the full shape of the channel base current while some of the typical inverse procedure algorithms only consider the channel base current at selected frequency samples. In addition, the current behaviour along the lightning channel can be evaluated by using the proposed method based on the measured electromagnetic fields without using any special current model as a basic assumption as opposed to previous methods where the current model has to be clear.

Also, the proposed method considers all the electromagnetic field components while some inverse procedure algorithms are simplified just for the radiation components of fields at far distances from the lightning channel. In most of the commonly used previous methods, the average value of the return stroke current velocity is a basic assumption while it is an unknown parameter in the proposed method and it is
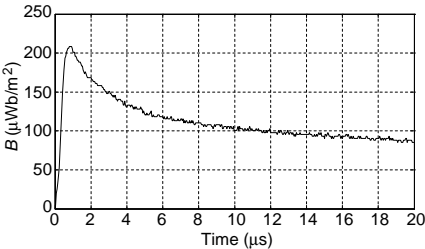
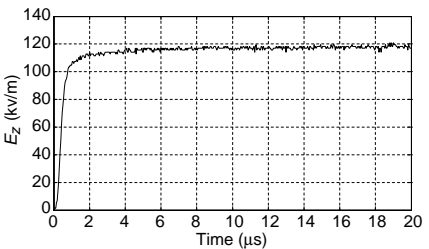**Figure 3.** The measured magnetic flux density at 15 m distance from the triggered lightning channel.

Figure 4. The measured vertical electric field at 15 m distance from the triggered lightning channel.

Table 1. The evaluated channel base current parameters based on measured electromagnetic fields.

	i_{01} (kA)	Γ_{11} (µs)	Γ_{12} (µs)	i_{02} (µs)	Γ_{21} (µs)	Γ_{22} (µs)	n_1	n_2
The evaluated current based on unknown model	14.81	0.244	2.77	6.86	4.18	40.66	2	2

evaluated based on the measured electromagnetic fields. Figures 3 and 4 illustrate the measured magnetic flux density and vertical electric field, respectively based on the geometry of the sensors as shown in Figure 2.

The evaluated current parameters based on the proposed method are tabulated in Table 1. Also, the evaluated channel base current based on the current parameters from Table 1 is illustrated in Figure 5.

Figure 5 illustrates that the peaks of the evaluated channel base currents are at about 15.9 kA. The value of the evaluated peaks can be generally examined by Ampere's law at a close distance (magnetostatics component) from the lightning channel as defined in Equation (16):

$$I_{peak} = \frac{2 \cdot \pi \cdot r \cdot B_{peak}}{\mu_0} \tag{16}$$

The estimated value of the current peak based on Equation (16) is
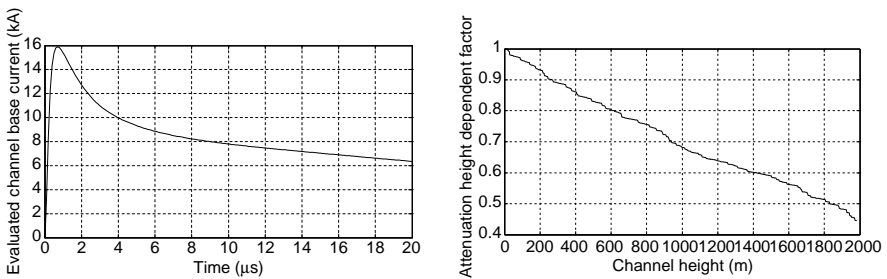
Figure 5. The evaluated channel base current based on current parameters from Table 1.

Figure 6. The behavior of evaluated attenuation height dependent factors versus temporary height changes along lightning channel.
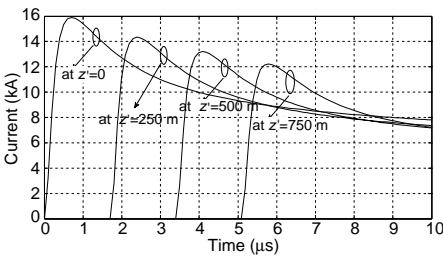

Figure 7. The evaluated return stroke current at different heights along lightning channel.

about 15.375 kA when the values $r = 15$ m and $B_{peak} = 205 \frac{\mu Wb}{m^2}$ are substituted into Equation (16). Note that the peak of the magnetic flux density at $r = 15$ m is obtained from Figure 3. A comparison between the current peak from Figure 5 and the estimated current peak based on Ampere's law confirms the evaluated current peak is within an acceptable range. Figure 6 illustrates the behaviour of the attenuation height dependent factors at different heights along a lightning channel. Furthermore, Figure 7 shows the current wave shapes at those different heights along a lightning channel. It is important to mention that the average value of the velocity along a lightning channel is determined to be 1.4752×10^8 m/s.

Furthermore, the simulated magnetic flux density at $r = 30$ m is compared to the corresponding measured field as shown in Figure 9 where the simulated field based on evaluated currents is obtained from the proposed method using measured fields at $r = 15$ m as illustrated in Figure 8.
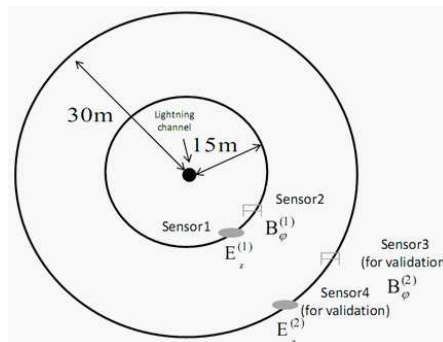
Figure 9 shows a good agreement between the wave shapes of the simulated magnetic flux density and the corresponding measured field at $r = 30$ m. In addition, a quantitative comparison between the simulated field and the corresponding measured field based on Figure 9 is listed in Table 2 as follows.

Table 2 shows that the simulated magnetic flux density based on the evaluated currents is much closer to the corresponding measured field at 30 m distance from the lightning channel while the average value of the difference percentage is about 3%. Moreover, the simulated vertical electric field at $r = 30$ m is compared with the corresponding measured field as shown in Figure 10, where the simulated field based on evaluated currents is obtained from the proposed method using

Figure 8. The geometry of field sensors in triggered lightning experiment.

Table 2. The quantitative comparison between the simulated magnetic flux density and the corresponding measured field based on Figure 9.

Time (µs)	At peak point	1	2	4	6	8	10
Measured magnetic flux density $(\frac{\mu Wb}{m^2})$	105	102.5	86.8	67.1	61	58	55
Simulated magnetic flux density $(\frac{\mu Wb}{m^2})$	101	100.5	84.8	66.5	59	55.5	52.5
Difference percent (%)	3.8	1.9	2.3	0.9	3.2	4.3	4.5
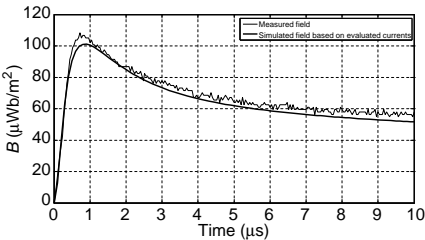
Figure 9. Comparison between the simulated magnetic flux density using evaluated currents and the corresponding measured field at $r_2 = 30$ m.
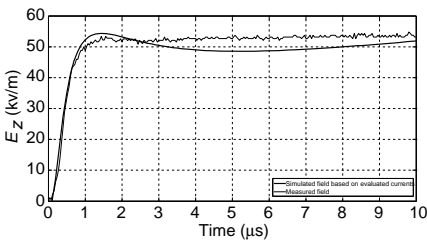

Figure 10. Comparison between the simulated vertical electric filed using evaluated currents and the corresponding measured field at $r_2 = 30$ m.

measured fields at $r = 15$ m (refer Figure 8 for the experimental arrangement).

Figure 10 illustrates a good agreement between the simulated vertical electric field and the corresponding measured field at $r = 30$ m while the difference between them can be due to the error of fields sensor and recorder, the angle of real channel with respect to vertical axis and the variation of return stroke velocity along lightning channel. In this study, the lightning is assumed to be as a vertical channel with a constant value of velocity along lightning channel.

Table 3. The quantitative comparison between the simulated vertical electric field and the corresponding measured field based on Figure 10.

Time (µs)	1.5 (First peak)	1	2	4	6	8	10
Measured vertical electric field (kv/m)	53	48.8	52	52.1	52.5	53.2	53.6
Simulated vertical electric field (kv/m)	54	52.2	53.2	49.2	49	50	51.9
Difference percent (%)	1.8	6.9	2.3	5.5	6.6	6	3.1

Likewise, a quantitative comparison between the simulated field and the corresponding measured field based on Figure 10 is tabulated in Table 3 as follows.

Table 3 shows the simulated vertical electric field based on the evaluated currents is in a good agreement with the corresponding measured field with the average value of the percentage difference is about 5%.

The proposed method considers all the field components directly in the time domain compared to previous methods that only supported the radiation components of the electromagnetic fields. Furthermore, the proposed method can evaluate the full shape of the channel base current compared to certain previous methods that can evaluate the current values only at selected frequency samples. On the other hand, the attenuation height dependent factors in the general form of the engineering current models are evaluated based on measured fields in the proposed method while in the previous methods a special current model is introduced as a basic assumption. Moreover, the required sensors in the proposed method are just two field sensors compared to some previous methods that need a greater number of field sensors while synchronization of the recorded fields from a large number of sensors is very complicated. The proposed method can evaluate current wave shapes related to a larger number of lightning occurrences based on the measured electromagnetic fields compared to direct current measurements while in the direct measurement technique the lightning

current can be measured by using triggered lightning or lightning strikes the tall towers. It is important to note that the radial distance between the striking point and the field sensors can be determined by a Lightning Location System.

5. CONCLUSION

In this paper, a numerical method for the evaluation of the lightning return stroke current using measured electromagnetic fields is proposed. The proposed method estimates the current wave shapes at different heights along a lightning channel directly in the time domain while it considers all components of the electromagnetic fields. Furthermore, it is applied to the measured fields from a triggered lightning experiment and the results are validated by comparison between the simulated fields obtained from the evaluated currents and the corresponding measured fields at an observation point. The results illustrate that the proposed method is in a good agreement with the measured fields. Last but not least, the proposed method is applicable to the measured fields due to the greater number of lightning occurrences compared to direct current measurements.

ACKNOWLEDGMENT

REFERENCES

1. Rakov, V., M. A. Uman, and K. J. Rambo, "A review of ten years of triggered-lightning experiments at Camp Blanding, Florida," *Atmospheric Research*, Vol. 76, 503–517, 2005.

2. Popov, M., S. He, and R. Thottappillil, "Reconstruction of lightning currents and return stroke model parameters using remote electromagnetic fields," *Journal of Geophysical Research*, Vol. 105, 24469–24481, 2000.

3. Andreotti, A., D. Assante, S. Falco, and L. Verolino, "An improved procedure for the return stroke current identification," *IEEE Transactions on Magnetics*, Vol. 41, 1872–1875, 2005.

4. Milewski, M. and A. Hussein, "Lightning return-stroke transmission line model based on CN tower lightning data and derivative of

Heidler function," *Canadian Conference on Electrical and Computer Engineering (CCECE)*, 2008.

5. Hussein, A., M. Milewski, W. Janischewskyj, F. Noor, and F. Jabbar, "Characteristics of lightning flashes striking the CN Tower below its tip," *Journal of Electrostatics*, Vol. 65, 307–315, 2007.

6. Kodali, V., V. Rakov, M. Uman, K. Rambo, G. Schnetzer, J. Schoene, and J. Jerauld, "Triggered-lightning properties inferred from measured currents and very close electric fields," *Atmospheric Research*, Vol. 76, 355–376, 2005.

7. Rachidi, F., J. Bermudez, M. Rubinstein, and V. Rakov, "On the estimation of lightning peak currents from measured fields using lightning location systems," *Journal of Electrostatics*, Vol. 60, 121–129, 2004.

8. Uman, M. A. and D. K. McLain, "Lightning return stroke current from magnetic and radiation field measurements," *Journal of Geophysical Research*, Vol. 75, 5143–5147, 1970.

9. Uman, M. A., D. K. McLain, and E. Krider, "The electromagnetic radiation from a finite antenna," *Amer. J. Phys.*, Vol. 43, 33–38, 1975.

10. Shoory, A., F. Rachidi, M. Rubinstein, R. Moini, and S. H. Sadeghi, "Analytical expressions for zero-crossing times in lightning return-stroke engineering models," *IEEE Transactions on Electromagnetic Compatibility*, Vol. 51, 963–974, 2009.

11. Rachidi, F. and C. Nucci, "On the Master, Uman, Lin, Standler and the modified transmission line lightning return stroke current models," *Journal of Geophysical Research*, Vol. 95, 20389–20393, 1990.

12. Thottappillil, R. and M. Uman, "Comparison of lightning return-stroke models," *Journal of Geophysical Research*, Vol. 98, 22903, 1993.

13. Andreotti, A., U. De Martinis, and L. Verolino, "An inverse procedure for the return stroke current identification," *IEEE Transactions on Electromagnetic Compatibility*, Vol. 43, 155–160, 2002.

14. Andreotti, A., F. Delfino, P. Girdinio, and L. Verolino, "An identification procedure for lightning return strokes," *Journal of Electrostatics*, Vol. 51, 326–332, 2001.

15. Andreotti, A., F. Delfino, P. Girdinio, and L. Verolino, "A field-based inverse algorithm for the identification of different height lightning return strokes," *The International Journal*

for Computation and Mathematics in Electrical and Electronic Engineering (COMPEL), Vol. 20, 724–731, 2001.

16. Rakov, V., "Characterization of lightning electromagnetic fields and their modeling," *14th Int. Zurich Symposium on Electromagnetic Compatibility*, 3–16, Zurich, 2001.

17. Bizjaev, A., V. Larionov, and E. Prokhorov, "Energetic characteristics of lightning channel," *20th Int. Conf. Lightning Protection*, 1.1, Switzerland, 1990.

18. Dubovoy, E., M. Mikhailov, A. Ogonkov, and V. Pryazhinsky, "Measurement and numerical modeling of radio sounding reflection from a lightning channel," *Journal of Geophysical Research*, Vol. 100, 1497–1502, 1995.

19. Dubovoy, E., V. Pryazhinsky, and G. Chitanava, "Calculation of energy dissipation in lightning channel," *Meteorologiya i Gidrologiya*, Vol. 2, 4–45, 1991.

20. Podgorski, A. S. and J. A. Landt, "Three dimensional time domain modelling of lightning," *IEEE Transactions on Power Delivery*, Vol. 2, 931–938, 1987.

21. Moini, R., B. Kordi, G. Rafi, and V. Rakov, "A new lightning return stroke model based on antenna theory," *Journal of Geophysical Research*, Vol. 105, 29693–29702, 2000.

22. Moini, R., S. Sadeghi, and B. Kordi, "An electromagnetic model of lightning return stroke channel using electric field integral equation in time domain," *Engineering Analysis with Boundary Elements*, Vol. 27, 305–314, 2003.

23. Gardner, R. L., *Lightning Electromagnetics,* Hemisphere Publishing, New York, 1990.

24. Visacro, S. and A. De Conti, "A distributed-circuit return-stroke model allowing time and height parameter variation to match lightning electromagnetic field waveform signatures," *Geophysical Research Letters*, Vol. 32, 2005.

25. Mattos, M. A. F. and C. Christopoulos, "A model of the lightning channel, including corona, and prediction of the generated electromagnetic fields," *Journal of Physics D: Applied Physics*, Vol. 23, 40, 1990.

26. Gomes, C. and V. Cooray, "Concepts of lightning return stroke models," *IEEE Transactions on Electromagnetic Compatibility*, Vol. 42, 82–96, 2000.

27. Cooray, V., "On the concepts used in return stroke models applied in engineering practice," *IEEE Transactions on Electromagnetic Compatibility*, Vol. 45, 101–108, 2003.

28. Cooray, V. and V. Rakov, "A current generation type return stroke model that predicts the return stroke velocity," *Journal of Lightning Research*, Vol. 1, 32–39, 2007.

29. Cooray. V., *The Lightning Flash,* IET Press, 2003.

30. Rakov, V. and M. Uman, "Review and evaluation of lightning return stroke models including some aspects of their application," *IEEE Transactions on Electromagnetic Compatibility*, Vol. 40, 403–426, 1998.

31. Diendorfer, G. and M. Uman, "An improved return stroke model with specified channel-base current," *Journal of Geophysical Research — Atmospheres*, Vol. 95, 13621–13644, 1990.

32. Izadi, M., M. Z. Ab Kadir, C. Gomes, and W. F. Ahmad, "Analytical expressions for electromagnetic fields associated with the inclined lightning channels in the time domain," *Electric Power Components and Systems*, Vol. 40, 414–438, 2012.

33. Izadi, M., M. Z. Ab Kadir, C. Gomes, and W. F. Ahmad, "An analytical second-FDTD method for evaluation of electric and magnetic fields at intermediate distances from lightning channel," *Progress In Electromagnetic Research*, Vol. 110, 329–352, 2010.

34. Izadi, M., M. Z. Ab Kadir, and C. Gomes, "Evaluation of electromagnetic fields associated with inclined lightning channel using second order FDTD-hybrid methods," *Progress In Electromagnetics Research*, Vol. 117, 209–236, 2011.

35. Izadi, M., M. Z. Ab Kadir, C. Gomes, and W. F. Ahmad, "Numerical expressions in time domain for electromagnetic fields due to lightning channels," *International Journal of Applied Electromagnetics and Mechanics*, Vol. 37, 275–289, 2011.

36. Kreyszig, E., *Advanced Engineering Mathematics,* Wiley-India, 2007.

37. Sadiku, M. N. O., *Numerical Technique in Electromagnetics,* CRC Press, LLC, 2001.

38. Lee, Y.-G., "Electric field discontinuity-considered effective-permittivities and integration-tensors for the three-dimensional finite-difference time-domain method," *Progress In Electromagnetics Research*, Vol. 118, 335–354, 2011.

39. Engelbrecht, A. P., *Fundamentals of Computational Swarm Intelligence,* 1st Edition, Wiley Chichester, UK, 2005.

40. Clerc, M., *Particle Swarm Optimization,* Wiley-ISTE, 2006.

41. Robinson, J. and Y. Rahmat-Samii, "Particle swarm optimization in electromagnetics," *IEEE Transactions on Antennas and Propagation*, Vol. 52, 397–407, 2004.

42. Zaharis, Z. D. and T. V. Yioultsis, "A novel adaptive beamforming technique applied on linear antenna arrays using adaptive mutated boolean PSO," *Progress In Electromagnetics Research*, Vol. 117, 165–179, 2011.

43. Zhang, Y., S. Wang, and L. Wu, "A novel method for magnetic resonance brain image classification based on adaptive chaotic PSO," *Progress In Electromagnetics Research*, Vol. 109, 325–343, 2010.

44. Zaharis, Z. D., K. A. Gotsis, and J. N. Sahalos, "Adaptive beamforming with low side lobe level using neural networks trained by mutated boolean PSO," *Progress In Electromagnetics Research*, Vol. 127, 139–154, 2012.

45. Li, Y., S. Sun, F. Yang, and L. J. Jiang, "Design of dual-band slotted patch hybrid couplers based on PSO algorithm," *Journal of Electromagnetic Waves and Applications*, Vol. 25, Nos. 17–18, 2409–2419, 2011.

46. Wang, D., H. Zhang, T. Xu, H. Wang, and G. Zhang, "Design and optimization of equal split broadband microstrip Wilkinson power divider using enhanced Particle Swarm Optimization algorithm," *Progress In Electromagnetics Research*, Vol. 118, 321–334, 2011.

47. Wang, J., B. Yang, S. H. Wu, and J. S. Chen, "A novel binary particle swarm optimization with feedback for synthesizing thinned planar arrays," *Journal of Electromagnetic Waves and Applications*, Vol. 25, Nos. 14–15, 1985–1998, 2011.